IOP Conf. Series: Materials Science and Engineering **365** (2018) 032068 doi:10.1088/1757-899X/365/3/032068

Optimization of Structural Parameters of Cement Composites with High Wear Resistance

Natalya Makarova[1,2] and Marina Polonik[1,2]

[1] Institute of Automation and Control Processes of Far Eastern Branch of RAS, Radio str. 5, 690041 Vladivostok, Russian Federation
[2] Far Eastern Federal University, Sukhanova str. 8, 690950 Vladivostok, Russian Federation
E-mail: maknat@bk.ru

Abstract. Within the model of the mechanics of contact interaction and on the basis of the experimental data there has been examined a number of tasks that allow us to determine the dependence of the wear resistance of composite materials from changes in their structural parameters. The solutions presented in integral form include both geometric parameters of hardened areas and tribological properties of the materials. Using these solutions, the structure of cement compositions was optimized by application of the numerical experiment and response surface methodology. Optimum parameters of the wear surface for the production of high-abrasion-resistance materials were found which agree with the results of experimental data.

1. Introduction

The granular cement composites are widely used as structural and protective materials in engineering structures, which surfaces are subject to abrasion. In the wear process of such heterogeneous materials the softer elements is destructed, whereas the harder elements is exposed. This may lead to loss of the effective thickness changes of structures that must be considered in predicting their life cycle.

In the simulation of such processes for the construction composites we should take into account the heterogeneity of the materials and their complex structure. The heterogeneity of materials, such as geometrical and mechanical, influence on the operation of the character of the state of stress up to failure. Considering heterogeneity of materials and their complex structure requires special formulations of the problems [1-4]. Thus, the most acceptable here is the use of instruments of mechanics of frictional interaction [1, 2], which allow us to take into account both complicated boundary conditions, the heterogeneity of the bodies and form change under friction and the surface microstructure, with the definition of stress in the contact area and surface layers. It should be noted that the application of theoretical and experimental methods of contact mechanics under modelling the cement composites, is difficult due to structural features, as compared with metal, ceramics and others. Thus, for a long time the study of abrasion resistance of such materials is carried out experimentally. So far in accepted engineering practice, the corresponding choice of compositions of the heterostructure and concrete mix is based on the results of costly and labor-intensive experiments [5-7].

The aim of this study is to consider the optimization problem, allowing us to determine the dependence of the strength properties of composite materials with a change in their structural parameters, based on the obtained experimental data and use of developed in this paper model of frictional interaction [8-10]. The result of optimization should be the minimum change in the shape of

abraded surface which is described by two functions, which is also dependent on several independent variables. Finding an optimal values to variables for both functions is a mathematically demanding task. This problem can be solved by the application of the Multiple Response Optimization procedure on the basis of the numerical experiment. As a result, the obtained data should allow us to formulate recommendations for the selection of the composition and technological parameters of composites with high strength and wear resistance in engineering practice.

2. Model

2.1 Major model relations in a steady mode of abrasion

To simulate the process of abrasion of construction composites we will use mathematical tools of the mechanics of frictional interaction [2]. To analyze the changes of contact pressures within a certain period of time and change of the surface form of half-space under abrasion of elastic half-space infinite die with a flat base we will use the system of equations [2]:

$$u_z(x,y,t) = A[p(x,y,t)],$$
$$\frac{d\omega_*}{dt} = K_\omega(x,y)\,p^\alpha(x,y,t)V_\infty^\beta(x,y,t), \qquad \iint\limits_\Omega p(x,y,t)dxdy = P(t), \tag{1}$$
$$u_z(x,y,t)+\omega_*(x,y,t) = D(t) - f(x,y,t),$$

where $u_z(x,y,t)$ and $\omega_*(x,y,t)$ – respectively the total elastic and the abrasion surfaces of the interacting bodies which have an initial shape $f_i(x,y)$; $p(x,y,t)$ – pressure on the contact area; α and β – materials parameters. For heterogeneous and hardened heterogeneous surfaces it is characteristic $K_\omega = K_\omega(x,y)$ that the abrasion ratio belongs to the class of piecewise constant functions:

$$K_\omega(x,y) = \begin{cases} K_{\omega_1}, & (x,y) \in \Omega \setminus \omega \\ K_{\omega_2}, & (x,y) \in \omega \end{cases}. \tag{2}$$

Under the conditions of existence of steady-state abrasion, i.e. provided that the speed of convergence of the interacting bodies under load $dD(t)/dt$ (or the magnitude of the normal load $P(t)$) tends towards a constant value D_∞ (or P_∞) when $t \to +\infty$, with the relative speed of sliding surfaces $V(x,y,t) = V(x,y)$ and the contact area $\Omega(t) = \Omega$ is also independent of time, we get the following steady contact pressure distribution:

$$p_\infty(x,y) = p^*\left[\frac{D_\infty (V^*)^\beta}{K_\omega(x,y)V^\beta(x,y)}\right]^{1/\alpha}, \tag{3}$$

where V^* and p^* – some characteristic values of speed and pressure.

Given the asymptotic value P_∞ of the normal load, D_∞ is determined from the third equation (1):

$$D_\infty = \frac{P_\infty^\alpha}{(p^*)^\alpha (V^*)^\beta}\left[\iint\limits_\Omega \frac{dxdy}{K_\omega^{1/\alpha}(x,y)V^{\beta/\alpha}(x,y)}\right]^{-\alpha}. \tag{4}$$

The established form $f_\infty(x,y)$ of the worn surface of the half-space corresponding to the contact pressure $p_\infty(x,y)$, is as follows:

$$f_\infty(x,y) = A[p_\infty(x,y)] = A\left[\left(\frac{(p^*)^\alpha (V^*)^\beta D_\infty}{K_\omega(x,y)V^\beta(x,y)}\right)^{1/\alpha}\right]. \tag{5}$$

Thus, the established form depends on the abrasion rate $K_\omega(x,y)$ and the nature of the die movement: function $V(x,y)$.

Operator A for half-space:

$$A[p(x,y,t)] = \frac{(1-\nu^2)}{\pi E}\iint_\Omega p(x',y',t)\varphi(x',y',x,y)dx'dy', \tag{6}$$

where $\varphi(x',y',x,y) = \left[(x-x')^2+(y-y')^2\right]^{-1/2}$, E – Young's modulus, ν – Poisson's ratio.

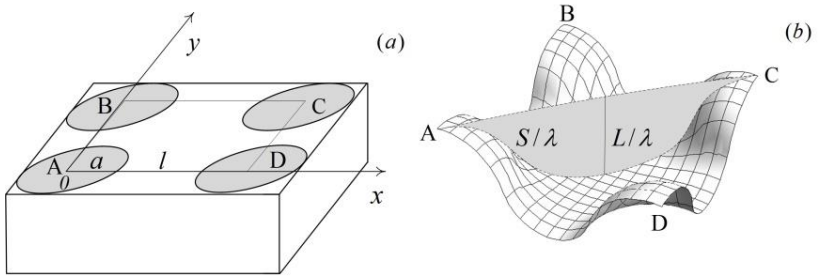

Figure 1. A square area of contact with the hardened area (circle radius a) (*a*), surface after abrasion (*b*); S – diagonal cross sectional area, and L – the amplitude of the abraded surface (*b*)

2.2 The dependence of the tribological characteristics from the geometric shape of the strengthened zone

Let's consider the abrasion of the elastic region by the endless die with a flat base ($f_0(x,y)=0$) which are moving progressively in opposite directions over the $z=0$ surface area. The square contact region Ω comprises of the hardened and non-hardened areas (Figure 1, *a*). The hardened area ω is a circle with a radius a, which are located in the tops of the initial contact area ABCD. We assume that the null point of the coordinate system is located in the center of the lower left hardened areas. The distance between the centers of the hardened areas, lying on one axis is equal to l. The pressure applied to the worn surface and the abrasion rate will be assumed to be constant: a steady mode.

We introduce the dimensionless parameters $m = K_{\omega_2}/K_{\omega_1}$ and $\tilde{a} = a/l$ characterizing the degree of hardening, respectively, and the relative size of the hardened area: $0 < \tilde{a} \le 0.5$ and $m_0 \le m < 1$, where m_0 – the minimum limit value determined by hardening technology.

Using formulas (3)–(4) steady pressure distribution is as follows:

$$\frac{p_\infty(x,y)}{p^*} = \begin{cases} \bar{p}_1, & (x,y)\in\Omega\setminus\omega \\ \bar{p}_2, & (x,y)\in\omega \end{cases}. \tag{7}$$

$$\bar{p}_1 = \frac{1}{(1+\tilde{S}_\omega m_2)}\left(\frac{P_\infty}{p^* l^2}\right), \quad \bar{p}_2 = \left(\frac{1}{m(1+\tilde{S}_\omega m_2)^\alpha}\right)^{1/\alpha}\left(\frac{P_\infty}{p^* l^2}\right), \quad m_2 = \frac{1}{m^\alpha}-1, \tag{8}$$

P_∞ – asymptotic value of the load on the region; $\tilde{S}_\omega$ takes values $\pi\tilde{a}^2$.

In the steady abrasion mode the surface form at a known pressure distribution (7) is obtained from equations (5)–(6):

$$\tilde{f}_\infty(x,y) = \frac{f_\infty(x,y)}{l} = \frac{1}{l}\left(\iint_\omega \Delta\bar{p}\,\varphi(x',y',x,y)dx'dy' + \iint_\Omega c_1\varphi(x',y',x,y)dx'dy'\right),$$

$$\Delta\bar{p} = \frac{1-\nu^2}{\pi E}\, p^*(\bar{p}_2 - \bar{p}_1) = \frac{1-\nu^2}{\pi E}\frac{P_\infty}{l^2}\frac{m_2}{1+\tilde{S}_\omega m_2}, \tag{9}$$

$$c_1 = \frac{1-\nu^2}{\pi E}\, p^*\bar{p}_1 = \frac{1-\nu^2}{\pi E}\frac{P_\infty}{l^2}\frac{1}{1+\tilde{S}_\omega m_2},$$

$$f_1(x,y) = \frac{1-\nu^2}{\pi E}\frac{P_\infty}{l^3}\frac{m_2}{1+\tilde{S}_\omega m_2}\iint_\omega \varphi(x',y',x,y)dx'dy'. \tag{10}$$

Transition of the surface integral (10) to the repeated integral allows us to search the integral solution in the form:

$$f_1(x,y) = \frac{1-\nu^2}{\pi E}\frac{P_\infty}{l^3}\frac{m_2}{1+\pi\tilde{a}^2 m_2}\times(W(x,y)+W(x,y-l)+W(x-l,y)+W(x-l,y-l)), \tag{11}$$

where

$$W(x,y) = G\left(\sqrt{x^2+y^2}, \arctan(y/x)\right) = G(r,\theta).$$

The transition to the polar coordinate system (r,θ) is implemented for more foreseeable solution:

$$G(r,\theta) = \int_0^{2\pi} d\theta_1 \int_0^{\tilde{a}} r_1\varphi(r_1\cos\theta_1, r_1\sin\theta_1, r\cos\theta, r\sin\theta)dr_1. \tag{12}$$

From (12) we obtain

$$G(r,\theta) = |a-r|\left(E_1\left[\frac{\theta}{2}, \frac{-4ar}{(a-r)^2}\right] - E_1\left[\frac{\theta}{2}-\pi, \frac{-4ar}{(a-r)^2}\right]\right) + \tag{13}$$

$$+\frac{(a^2-r^2)}{|a-r|}\left(F_1\left[\frac{\theta}{2}, \frac{-4ar}{(a-r)^2}\right] - F_1\left[\frac{\theta}{2}-\pi, \frac{-4ar}{(a-r)^2}\right]\right),$$

where $E_1[\phi, n] = \text{Elliptic}E[\phi, n]$ – the elliptic integral of the second kind, $F_1[\phi, n] = \text{Elliptic}F[\phi, n]$ – the elliptic integral of the first kind.

In Figure 1, *b* is a graph of the surface at one period $f_1(x,y)/\lambda$, where $\lambda = (1-\nu^2)P_\infty/(\pi E l^2)$, in the area ABCD enclosed between the peaks of the hardened areas.

To determine the tribological characteristics of the surface, we write down the equation (11) along a straight line $x = y$:

$$\Phi(\xi) = f_1\left(\frac{\xi}{\sqrt{2}}, \frac{\xi}{\sqrt{2}}\right), \quad \xi = \frac{x}{l} = \frac{y}{l}, \quad 0 \le \xi \le \sqrt{2}. \tag{14}$$

Then, according to (11)–(13), taking into account (14), we obtain:

$$\Phi(\xi) = \frac{1-\nu^2}{\pi E}\frac{P_\infty}{l^2}\frac{m_2}{1+\pi\tilde{a}^2 m_2}\times\left(|a-\xi|\left(E_1\left[\frac{\pi}{8}, \xi_1\right] + E_1\left[\frac{7\pi}{8}, \xi_1\right]\right) + \frac{a^2-\xi^2}{|a-\xi|}\left(F_1\left[\frac{\pi}{8}, \xi_1\right] + F_1\left[\frac{7\pi}{8}, \xi_1\right]\right) + \right.$$

$$+\left|\sqrt{2}+a-\xi\right|\left(E_1\left[\frac{\pi}{8}, \xi_2\right] + E_1\left[\frac{7\pi}{8}, \xi_2\right]\right) + \left(a+\xi-\sqrt{2}\right)\left(F_1\left[\frac{\pi}{8}, \xi_2\right] + F_1\left[\frac{7\pi}{8}, \xi_2\right]\right) + \tag{15}$$

$$\left. +\left|a-\sqrt{1-\sqrt{2}\xi+\xi^2}\right|\left(E_1[\pi-\gamma_1, \xi_3] + E_1[\gamma_1, \xi_3] + E_1[\pi-\gamma_2, \xi_3] + E_1[\gamma_2, \xi_3]\right) + \right.$$

$$+\frac{a^2-\left(1-\sqrt{2}\xi+\xi^2\right)}{\left|a-\sqrt{1-\sqrt{2}\xi+\xi^2}\right|}\left(F_1[\pi-\gamma_1,\xi_3]+F_1[\gamma_1,\xi_3]+F_1[\pi-\gamma_2,\xi_3]+F_1[\gamma_2,\xi_3]\right)\Big),$$

The following notation is used in the formula (15):

$$\xi_1=\frac{-4a\xi}{(a-\xi)^2},\ \xi_2=\frac{-4a\left(\xi-\sqrt{2}\right)}{\left(\sqrt{2}+a-\xi\right)^2},\ \xi_3=\frac{-4a\sqrt{1-\sqrt{2}\xi+\xi^2}}{\left(a-\sqrt{1-\sqrt{2}\xi+\xi^2}\right)^2},$$

$$\gamma_1=\frac{1}{2}\arctan\left(\frac{\xi}{\xi-\sqrt{2}}\right),\ \gamma_2=\frac{1}{2}\arctan\left(\frac{\xi-\sqrt{2}}{\xi}\right).$$

For easier determination of the amplitude and area of the diagonal section we carry out the transformation of the function $\Phi(\xi)$, transferring it to the null point of the coordinate system: $\Phi_1(\xi)=\Phi(\sqrt{2})-\Phi(\xi)$.

Taking into account the new function, the amplitude (L) and diagonal cross-sectional area (S) (Figure 1, *b*), are respectively calculated according to the formulas:

$$L=\Phi_1\left(\frac{\sqrt{2}}{2}\right),\quad S=\int_0^{\sqrt{2}}\Phi_1(\xi)d\xi. \tag{16}$$

3. Results and discussion

3.1 Numerical Optimization Using Experiment Design

Previous experimental studies confirmed that the strength of the cement matrix and coarse aggregate consumption are the most important structural parameters that affect the exploitation properties of cement composites [7]. The analysis of the developed model relations (16) have shown that by controlling the physical and geometrical parameters of the surface the material may be produced with a minimal degree of wear. Below Figure 2 shows graphs of amplitude dependence (L/λ) and area (S/λ) from the hardened areas under the given values $m=\{0.60;\ 0.75;\ 0.90\}$ and $\alpha=1$.

The minimum degree of the surface wear can be obtained by minimizing the value of both functions simultaneously. However, as can be seen in the Figure 2, the functions L/λ and S/λ have different increment signs within the selected interval. Moreover, the application of traditional mathematical optimization methods to these functions is difficult because of their cumbersomeness.

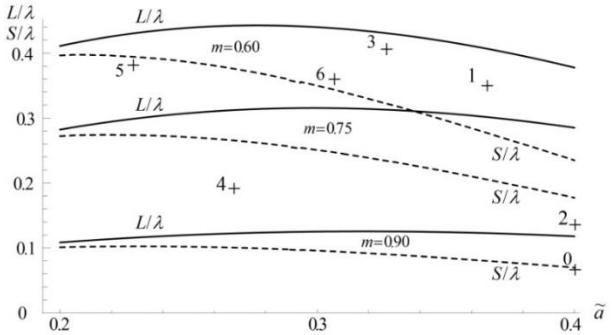

Figure 2. Dependences of the amplitude (L/λ) and area (S/λ) from the hardened areas $\tilde{a}$, for given values $m=\{0.60;0.75;0.90\}$, $\tilde{a}\in[0.2;0.4]$

On the basis of the developed model the relations the rotatable design of numerical experiment was created to optimize of technological and structured parameters. This plan should provide information on the impact of each factor on the studied values and the joint effect of the interaction of factors, as well as to apply the procedure of multiple optimizations.

In this experiment, there are two response variables: L – the amplitude of the abraded surface, and S – a diagonal cross-sectional area, defined by the relations (16).As a variable parameter X_1 we have accepted as a dimensionless geometric ratio of the radius of hardened area a to the distance between their centers l: $\tilde{a} = a/l$. As a variable parameter X_2 – the dimensionless ratio of the surface hardness of the matrix and the hard inclusions $m = K_{\omega_2}/K_{\omega_1}$, taking into account changes of the elastic modulus E. For different values $m = \{0.60; 0.75; 0.90\}$ we must take into account the corresponding to them modules of elasticity $E = \{25E/33;\ E;\ 37E/33\}$. The values L/λ and S/λ in Table 1 have been computed taking into account $E = \{25E/33;\ E;\ 37E/33\}$. The limit variability intervals for the X_1 and X_2 are taken based on fracto-graphic investigations of concrete surface abrasion with different composition [11]:

$$0.2 \le X_1 \le 0.4;\ 0.6 \le X_2 \le 0.9.$$

Other variable factors in (16) depending on the method and test conditions (coefficients α and β), loading conditions (value of the path length l, pressure P_∞) are taken as constants.

The experimental design and results of the numerical experiment are shown in Table 1.

Table 1. The matrix of planning and results of the experiment

No.	Parameters			
	$\tilde{a}$	m	L/λ	S/λ
1.	0.2	0.60	0.411042	0.39648210
2.	0.3	0.60	0.440046	0.34987320
3.	0.4	0.60	0.377749	0.23483250
4.	0.2	0.75	0.282195	0.27219870
5.	0.3	0.75	0.315445	0.25080520
6.	0.4	0.75	0.285093	0.17723150
7.	0.2	0.90	0.108371	0.10453260
8.	0.3	0.90	0.125076	0.09944544
9.	0.4	0.90	0.117822	0.07324552

Based on the rotatable composite design, each of the two factors ($\tilde{a}$ and m) were the most important variables for all of the analysis. STATGRAPHICS was used for realizing this design. The obtained results of the experimental design were evaluated at a 5% of significance and were analyzed by Standardized Pareto chart (Figure 3).

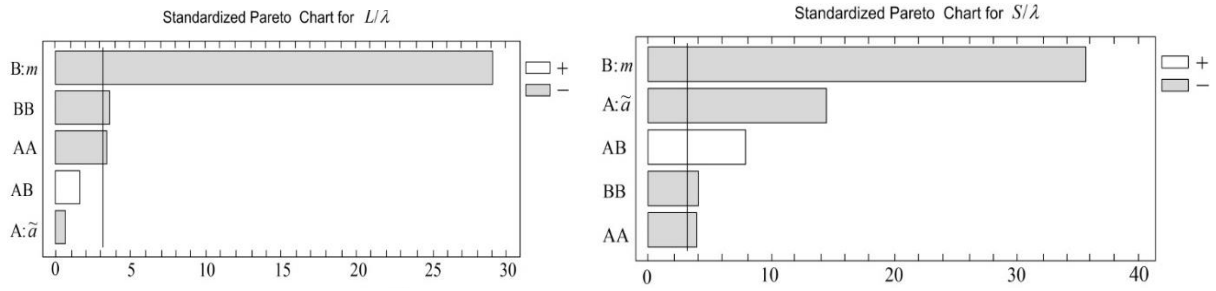

Figure 3. Influence of independent factors $\tilde{a}$, m on response functions: L/λ, S/λ

The vertical line on the plot judges the effects that are statistically significant. The bars, extending beyond the line, correspond to the effects that are statistically significant at the 95% confidence level. Furthermore, the positive or negative sign (corresponding to a black or white) response can be enhanced or reduced, respectively, when passing from the lowest to the highest level set for the specific factor. As Figure 3 shows, the hardness parameter m has the largest influence on a positive effect. In fact, by increasing of the matrix strength at the fixed geometrical concentration parameters, the wear resistance will increase. On the other hand, cost of material increases substantially at higher matrix strength. Therefore, both strength and geometrical parameters play an important role in the optimization process.

When a single function is being analyzed, the model analysis indicates areas in the design region where the process is likely to give desirable results, which is a relatively easy task (Figure 2). However, a function of more than one response can be used: the desirability function, which includes the researcher's priorities and desires on building the optimization procedure [12].

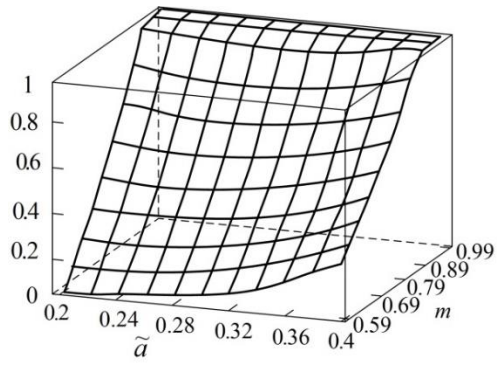

Figure 4. Resulting response of multiple optimization

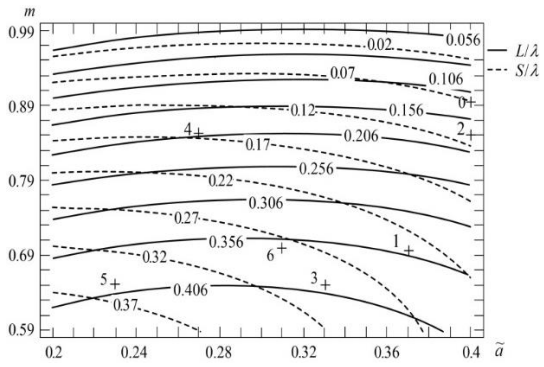

Figure 5. Resulting numerical overlay plot for L/λ and S/λ

Following the conditions and restrictions previously discussed, the optimization procedure was carried out and the response surfaces obtained for a given pair of factors is presented in Figure 4. When the number of response variables is small, contour plots for each response may be overlaid to show the optimum point graphically. Contour plots for each response were overlaid to show the optimum point graphically (+0), as shown in Figure 5. Analysis of the obtained response surface showed that the minimal values of the function L/λ = 0.1144 and S/λ = 0.069 are achieved at values of $\tilde{a}$ = 0.4, m = 0.90 at the examined interval. However, for engineering practice it is convenient to use the digitized graph (Figure 5), taking into account other technological parameters.

3.2 Experimental Investigation

In order to determine the dependency concrete's resistance to abrasion we conducted 6 series of experiments in which the concrete mix compositions differed in volume content of the coarse fraction, microsilica, superplasticizer, the water cement ratio, cement content. The test procedure met the requirements of GOST 13087–81. The abrasion resistance was evaluated as a weight loss of the sample ΔG (g/sm^2) and as a reduction in linear size Δh (mm). The tests were performed on a standard abrading wheel, and the total length of the path of the sample was 600 m (20 cycles to 30 m).

After testing the geometrical and physical parameters of the obtained surfaces were investigated. To determine the parameter $\tilde{a}$ the sizes of the bared grains of coarse aggregate a and the distance between their centers l were measured. The hardness of the aggregate and cement-sand matrix were

determined using the Poldi device. Hardening parameter was defined as $m = K_{\omega_2}/K_{\omega_1} = d_2/d_1$, where d_2, d_1 are the values of the obtained diameter on the metallic rod under the testing of the cement matrix and coarse aggregate respectively [7].

Table 2. Experimental results of abrasion test

No. series	Parameters			
	Δh, *mm*	ΔG, *g/sm*^{2}	m	$\tilde{a}$
1.	4.29	0.93	0.70	0.37
2.	3.46	0.90	0.85	0.41
3.	4.59	1.23	0.65	0.33
4.	3.62	0.91	0.85	0.27
5.	4.90	1.31	0.65	0.23
6.	4.44	0.97	0.70	0.31

The obtained experimental data are consistent with the results of numerical realization of the proposed model. On the Fig. 2 and Fig. 5, for comparison, there are given the points {1+, 2+, 3+, 4+, 5+, 6+} corresponding to the tribological characteristics of concrete samples of the series 1-6 (Table 2). Thus, the most wear-resistant was the concrete of the series 1 (Table 2). It has, in accordance with the model, the lowest L and S. On the contrary, the concrete of the series 5 (Table 2), for which out of the submitted samples the obtained L and S are maximal, showed the lowest wear resistance.

4. Conclusion

In this paper a multiple response surface methodology has been used to optimization of structural parameters of cement composites to minimize the degree of abrasive wear. The model of the frictional interaction mechanic developed to simulate the wear process of the stochastically heterogeneous surfaces was used as a basis for optimization.

The experimental study of the concrete samples with different structures was made. It allowed us to obtain the geometrical and physical parameters of the abraded surfaces and to find their influence on the resistance to abrasion. As result, good agreement is found between the computed and experimental values. Optimum value of structure parameters can be taken by using obtained resulting numerical overlay plot as a basis for following investigations.

5. References

[1] Goryacheva I G 1987 *Izvestiya RAN, Mekhanika Tverdogo Tela* vol 6 pp 62–68 (In Russian)
[2] Goryacheva I G 2001 *Mechanics of friction interaction* (Moskva: Nauka) (In Russian)
[3] Alexandrov V M 1982 *Izvestiya RAN, Mekhanika Tverdogo Tela* vol 4 pp 98–10 (In Russian)
[4] Galin L A 1977 J. Appl. Mech. vol 5(41) pp 807–812 (In Russian)
[5] Itoh Y, Yoshida A, Tsuchiya M and Katoh K 1988 *Proc. of offshore technology conf.* OTC 5687
[6] Saeki H, Asai Y, Izumi K and Takeuchi T 1988 *The 20th Marine Development Symposium, Japan*
[7] Makarova N V 2009 *Vestnik grazhdanskih inzhenerov* vol 3 pp 137–139 (In Russian)
[8] Makarova N V and Polonik M V 2012 *Proceedings of the International Offshore and Polar Engineering Conference* pp 67–71
[9] Makarova N V and Polonik M V 2013 *Applied Mechanics and Materials* vol 248 pp 355–360
[10] Makarova N V, Polonik M V and Rogachev E E 2012 *Bulletin of CSPU named after I.Ya. Yakovlev. Series: Mechanics of limit state. Problems of Nonlinear Mechanics and inelastic deformation of solids* vol 4(14) pp 164–173 (In Russian)
[11] Makarova N V 2013 *Applied Mechanics and Materials vol* 357 (Zurich: Trans Tech Publ) pp.

1259–1262
[12] Myers R H and Montgomery D C 1995 *Response Surface Methodology: Process and Product Optimization Using Designed Experiments* (New York: Wiley–Interscience)